Supporting information

for

Revealing the synergistic effect for Cu-Cu_2S during urea electrosynthesis

Yuhua Xie[a], Qi Xu[b], Shiao Zhu[c], Fang Luo[b*] and Zehui Yang[a,c*]

[a]College of Materials and Chemical Engineering, China Three Gorges University, Yichang 443002, P. R. China.

[b]State Key Laboratory of New Textile Materials & Advanced Processing Technology, College of Materials Science and Engineering, Wuhan Textile University, Wuhan 430200, P. R. China.

[c]Faculty of Materials Science and Chemistry, China University of Geosciences Wuhan, 388 Lumo RD, Wuhan, 430074, China.

Experimental section

Preparation of Cu_2S and Cu-Cu_2S: 2.5 mmol (0.6242 g) of $CuSO_4 \cdot 5H_2O$ was dissolved in 13 mL of deionized water, then 7 mL of thiourea ethylene glycol solution (0.5709 g of thiourea dissolved in 7 mL of ethylene glycol solution) was added dropwise to the copper sulfate solution. This was stirred at 500 r min^{-1} for 10 min, placed in an autoclave, reacted at 180 ℃ for 4 h, and the hydrothermal reaction sample was collected. The sample was repeatedly centrifuged and washed with deionized water and anhydrous ethanol, dried at 80℃ for 10 h to obtain Cu_2S. Then, 0.25 g of Cu_2S powder was ground and in a tube furnace (under 10% Ar/H_2 conditions) held at 450 ℃ for 8 h, cooled and ground to Cu-Cu_2S.

Fundamental characterization: XRD patterns were recorded using a Bruker D8 Advance diffractometer with Cu-Kα radiation (λ=1.5406 Å). The surface morphology was observed via a scanning electron microscope (SEM, SU8010). The elemental composition was determined by X-ray photoelectron spectroscopy (XPS, ESCALB 250) with an Al Kα X-ray source. TEM images were acquired using a Talos F200x microscope.

Electrochemical measurement: All electrochemical tests were performed at room temperature using a Gamry Reference 1000 electrochemical workstation in a three-electrode system, where a 3 mm-diameter glassy carbon electrode (GCE), a saturated calomel electrode (SCE), and a carbon rod served as the working, reference, and counter electrodes, respectively. The electrocatalytic activity for the nitrogen reduction reaction (NRR) was evaluated in an H-type electrochemical cell separated

by a Nafion 212 membrane, using a N_2-saturated 0.05 M H_2SO_4 solution as the electrolyte. Prior to use, the Nafion 212 membrane was pretreated as follows: boiled in ultrapure water for 1 h, heated in 5% H_2O_2 at 80℃ for 1 h, and finally boiled in 0.5 M H_2SO_4 for 2 h. Additionally, N_2 was purified with H_2SO_4 before being purged into the electrolyte. For urea electrosynthesis, 200 ppm KNO_3 were added to the catholyte with CO_2 purging. All potentials reported in this manuscript were converted to the reversible hydrogen electrode (RHE) scale using the equation: E (vs. RHE) = E (vs. SCE) + 0.0591 × pH + 0.244 V. The turnover frequency (TOF) value was estimated from the equation: $TOF_{catalyst}$ (s^{-1}) = i_{urea} (A cm^{-2})/{[density of Cu atoms in the catalyst (sites per cm^2)] * [1.602*10^{-19} (C per e-)] * [$2e^-/H_2$]}.

Faradaic Efficiency (FE) and Yield of Urea: The FE for urea electrosynthesis is defined as the charge used to produce urea divided by the total charge passing through the electrodes during electrolysis. Assuming 16 electrons are required to generate one urea molecule, the FE calculation formula is as follows:

$$FE_{urea}=(16*F*C_{urea}*V)/(Q*M_{Urea})$$

Where F is the Faraday constant (96485.3 C mol^{-1}), C_{urea} is the measured urea concentration (mg L^{-1}), V is the total electrolyte volume (mL), Q is the total charge passing through the working electrode (C), 16 is the number of electrons transferred in the reaction, and M_{Urea} is the molar mass of urea. The urea generation rate formula is:

$$R_{urea}=(C_{urea}*V)/(t*m*M_{Urea})$$

where C_{urea} is the measured urea concentration (mg L^{-1}), V is the total electrolyte volume (mL), t is the electrocatalytic operation time (h), m is the catalyst mass loaded

onto the electrode (g).

Faradaic Efficiency (FE) and Yield of Ammonia: The FE of ammonia electrolysis is defined as the charge used to produce NH_3 divided by the total charge passing through the electrode during electrolysis. Assuming eight electrons are required to generate one NH_3 molecule, the formula for calculating FE is as follows:

$$FE_{NH3}=(8*F*C_{NH3}*V)/(Q*M_{NH3})$$

where F is the Faraday constant (96485.3 C mol^{-1}), C is the measured ammonia concentration (mg L^{-1}), V is the total electrolyte volume (mL), Q is the total charge passing through the working electrode (C), 8 is the number of electrons transferred in the reaction, and M_{NH3} is the molar mass of ammonia.

$$R_{NH3}=(C_{NH3}*V)/(t*m*M_{NH3})$$

Where C_{NH3} is the measured urea concentration (mg L^{-1}), V is the total volume of the electrolyte (mL), t is the electrocatalytic operation time (h), m is the mass of catalyst loaded onto the electrode (g).

Faradaic Efficiency (FE) and Yield of NO_2^-

Formula for calculating the Faradaic efficiency of nitrite ions:

$$FE_{NO2-}=(2*F*C_{NO2-}*V)/(M_{NO2-}*Q)$$

Where F is the Faraday constant (96485.3 C mol^{-1}), C is the measured nitrite concentration (mg L^{-1}), V is the total electrolyte volume (mL), Q is the total charge passing through the working electrode (C), 2 electrons transferred in the reaction, and M_{NO2-} is the molar mass of nitrite.

$$R_{NO2-}=(C_{NO2}-*V)/(t*m*M_{NO2-})$$

Where C_{NO2-} is the measured urea concentration (mg L^{-1}), V is the total electrolyte volume (mL), t is the electrocatalytic operation time (h), m is the catalyst mass loaded onto the electrode (g).

DFT Calculations

All DFT calculations were performed using Vienna Ab Initio Simulation Package (VASP) in a spin-polarized mode. The exchange–correlation effect was estimated by Generalized Gradient Approximation Perdew-Burke-Ernzerhof (GGA-PBE) functionals. A plane wave basis with a cut off energy of 550 eV was used to expand the Kohn-Sham wave functions. Convergence criteria for geometry structures were set to be that residual energy and force were below 10^{-5} eV and -0.02 eV $Å^{-1}$, respectively. 3×3×1 gamma centered k-point grid was used to sample surfaces. The top two layers of the surfaces were fully relaxed during structural optimization.

The energy (E (ads)) of each primitive step is defined as:

$\Delta G\ (ads) = \Delta E_{DFT} + \Delta E_{ZPE} + T*\Delta S$

among ΔE_{DFT} is the binding energy obtained by DFT, and the zero-energy correction difference ΔE_{ZPE} and $T*\Delta S$ is calculated by vibration analysis.

Table S1. Comparison of the optimum urea yield rate and FE_{urea} for the recently reported urea electrocatalysts at ambient conditions.

Electrocatalyst	Electrolyte	Urea yield rate (mmol h^{-1} g_{cat}^{-1})	FE_{urea} (%)	Potential （V vs. RHE）	Ref.
Cu-Cu_2S	0.1M KNO_3 (CO_2)	**8.21**	**45.25**	**-0.40**	**This work**
Pd_1−TiO_2	0.1M KCO_3 (CO_2+N_2)	2.936	3.79	-0.5	1
Pd_1Cu_1−TiO_2		166.67	22.54	-0.5	
Fe(a)@C-Fe_3O_4/CNTs	0.1M KNO_3 (CO_2)	22.33	16.5	-0.65	2
CuRu-CBC	0.1M KNO_3 (CO_2)	6.574	68.94	-0.55	3
Fe^{II}-Fe^{III}OOH@$BiVO_4$-n	0.1M KNO_3 (CO_2)	13.8	11.5	-0.8	4
FeOOH		3.2	1.3		
$BiVO_4$		2.0	5.4		
$CuWO_4$	0.1M KNO_3 (CO_2)	1.64	70.1	-0.2	5
MoOx/C	0.1M KNO_3 (CO_2)	23.83	27.7	-0.6	6
VB_{12}-CNTs	0.1M KNO_3 (CO_2)	2.73	26.04	-0.5	7
$In(OH)_3$-S	0.1M KNO_3 (CO_2)	8.88	53.4	-0.6	8
PdCu/CBC	0.05M KNO_3 (CO_2)	12.72	59.7	-0.5	9
$CoRuN_6$	0.1M KNO_3 (CO_2)	8.98	25.31	-0.6	10

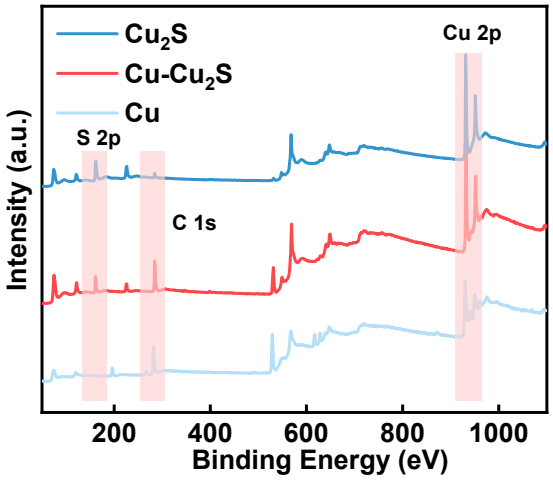

Figure S1 XPS survey scan of Cu, Cu_2S and Cu-Cu_2S.

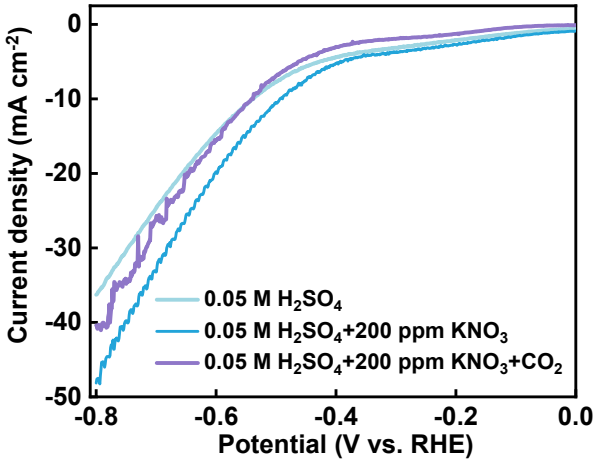

Figure S2 Polarization curves of metallic Cu before and after adding different substances to a 0.05 M H_2SO_4 electrolyte.

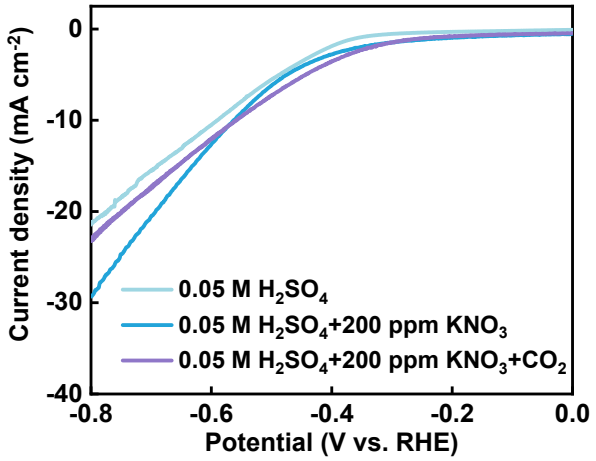

Figure S3 Polarization curves of metallic Cu_2S before and after adding different substances to a 0.05 M H_2SO_4 electrolyte.

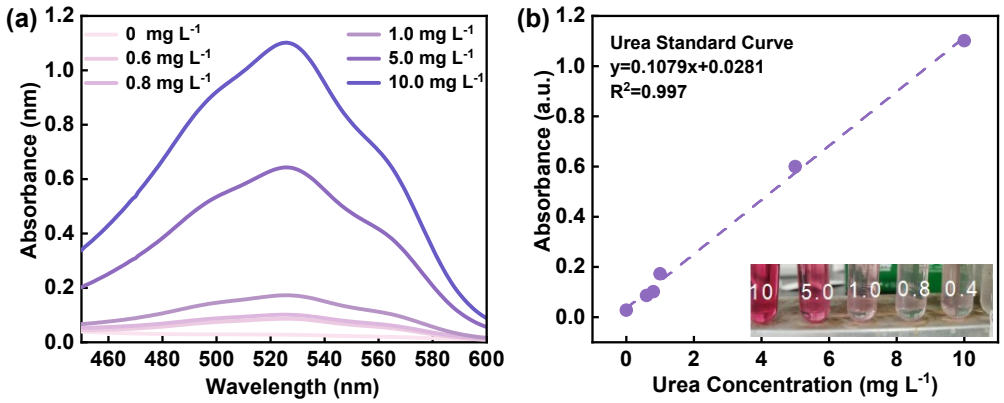

Figure S4 UV spectroscopies of urea with controlled concentrations using the diacetyl monoxime method and fitted standard curve.

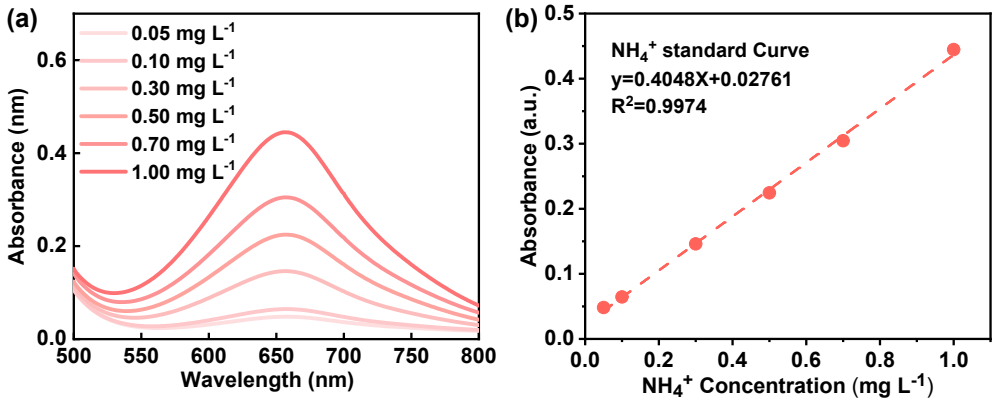

Figure S5 UV spectroscopies of NH_4^+ with controlled concentrations using the diacetyl monoxime method and fitted standard curve.

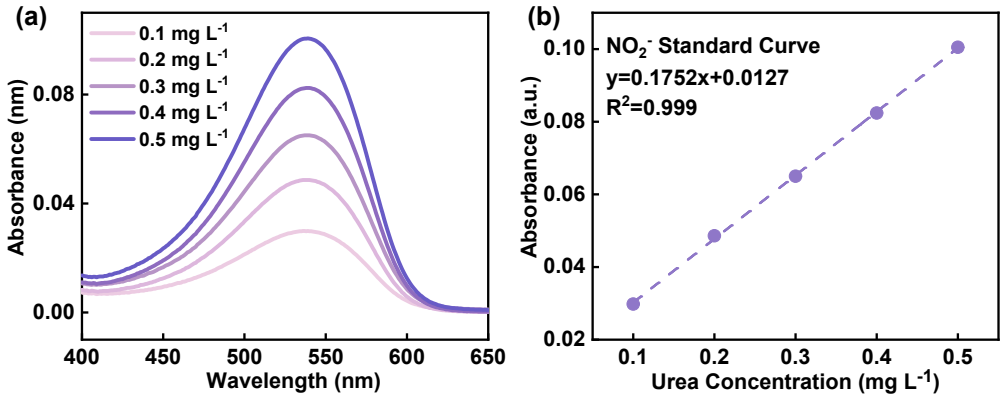

Figure S6 UV spectroscopies of NO_2^- with controlled concentrations using the diacetyl monoxime method and fitted standard curve.

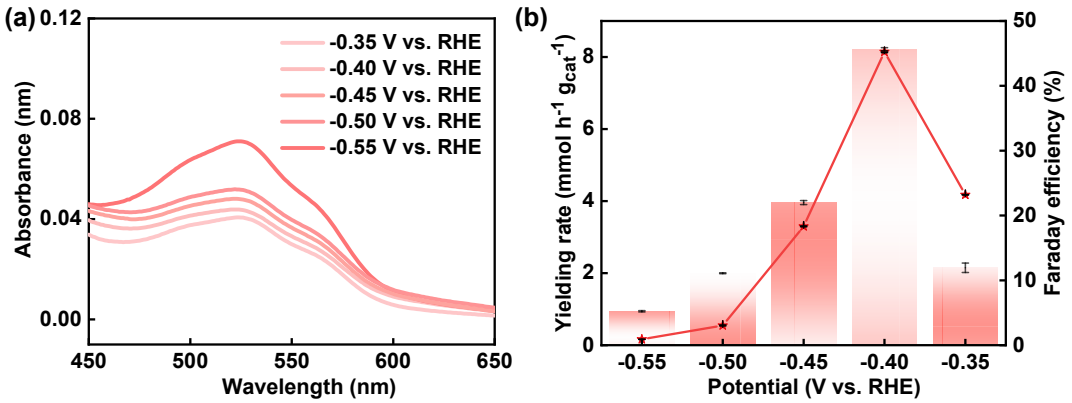

Figure S7 UV-vis spectroscopy of collected electrolyte at 525 nm and measured urea yield and Faradaic efficiency for Cu-Cu_2S.

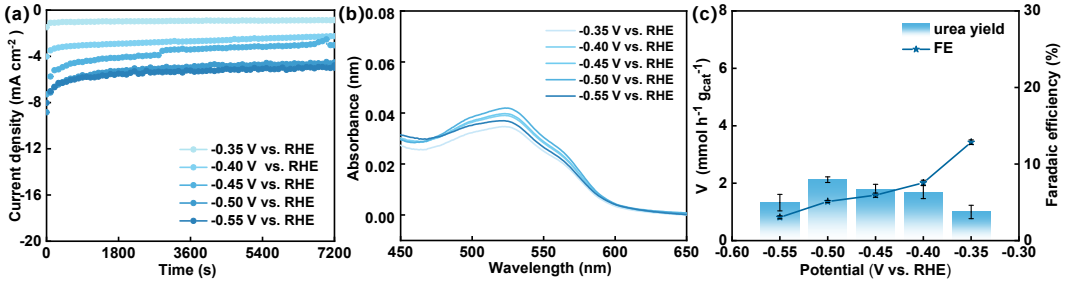

Figure S8 (a) i-t curves of Cu at different reduction potentials over 2 h, (b) UV-vis spectroscopy of collected electrolyte at 525 nm, and (c) measured urea yield and Faradaic efficiency.

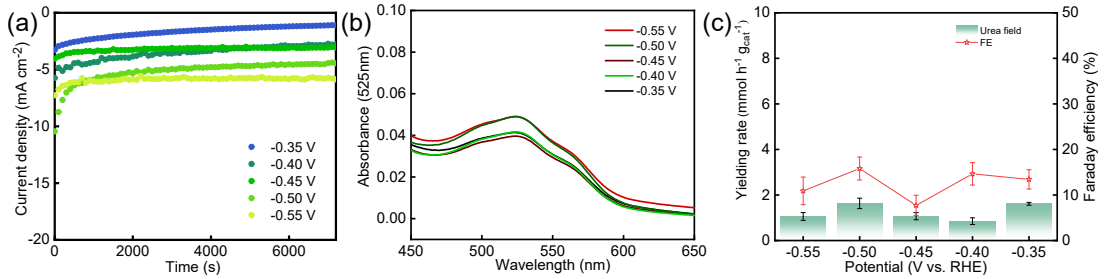

Figure S9 (a) i-t curves of Cu_2S at different reduction potentials over 2 h, (b) UV-vis spectroscopy of collected electrolyte at 525 nm, and (c) measured urea yield and Faradaic efficiency.

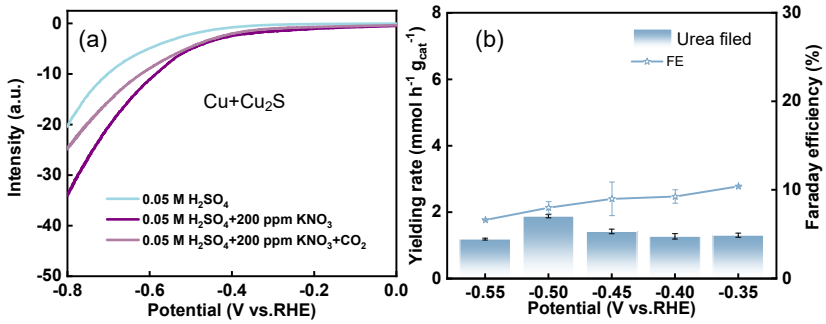

Figure S10 (a) Polarization curves of metallic Cu+Cu_2S before and after adding different substances to a 0.05 M H_2SO_4 electrolyte. (b) Calculated urea yield and Faradaic efficiency.

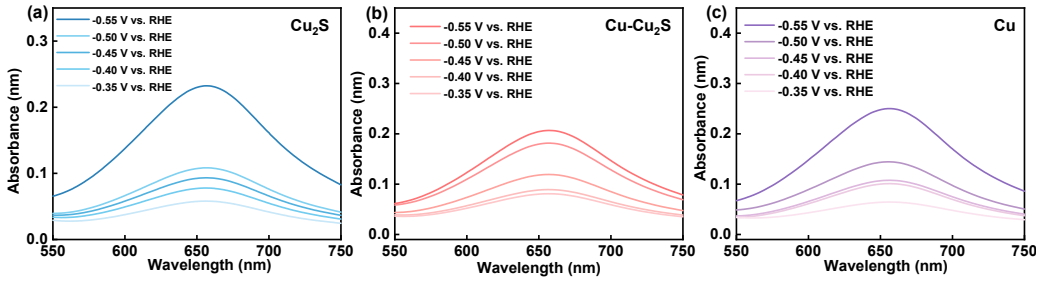

Figure S11 The UV-visible spectroscopy of Cu_2S (a), Cu-Cu_2S (b) and Cu (c) during electrochemical ammonia synthesis at 655 nm within the same duration.

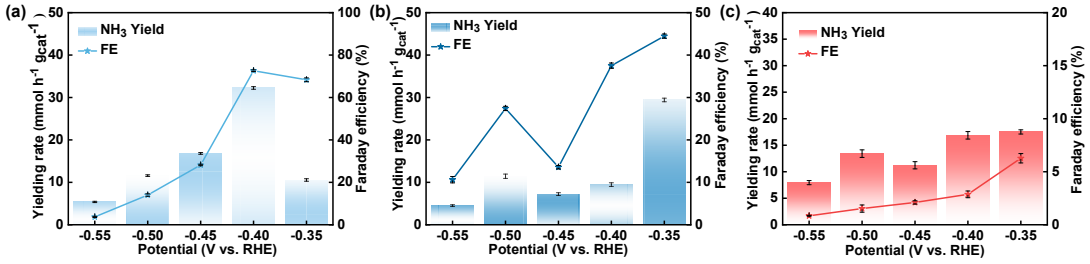

Figure S12 Ammonia yield and Faraday efficiency of (a) Cu, (b) Cu_2S, and (c) Cu-Cu_2S.

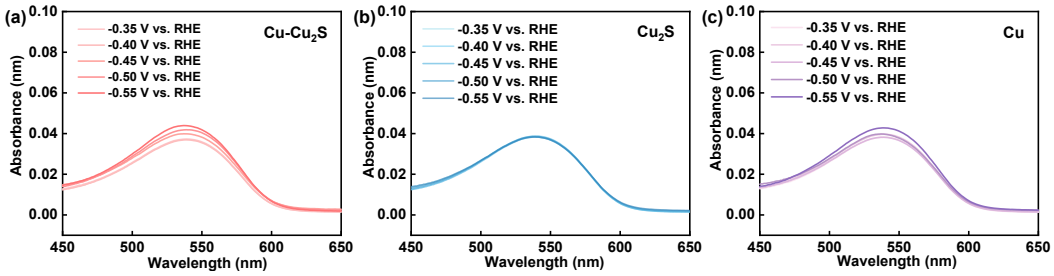

Figure S13 The UV-vis spectroscopy of Cu-Cu_2S (a), Cu_2S (b) and Cu (c) during electrochemical ammonia synthesis at 540 nm within the same duration.

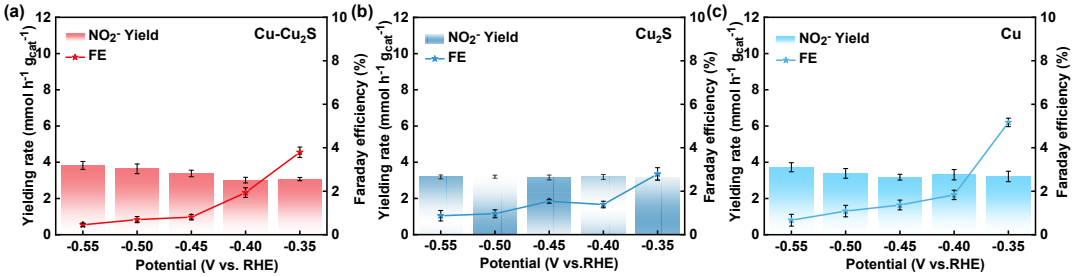

Figure S14 NO_2^- yield and Faraday efficiency of (a) Cu, (b) Cu_2S, and (c) Cu-Cu_2S.

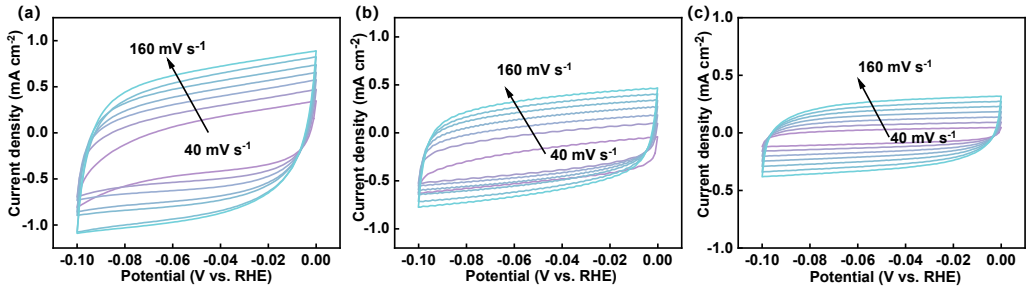

Figure S15 Cyclic voltammetry curves of Cu-Cu_2S (a), Cu_2S (b) and Cu (c).

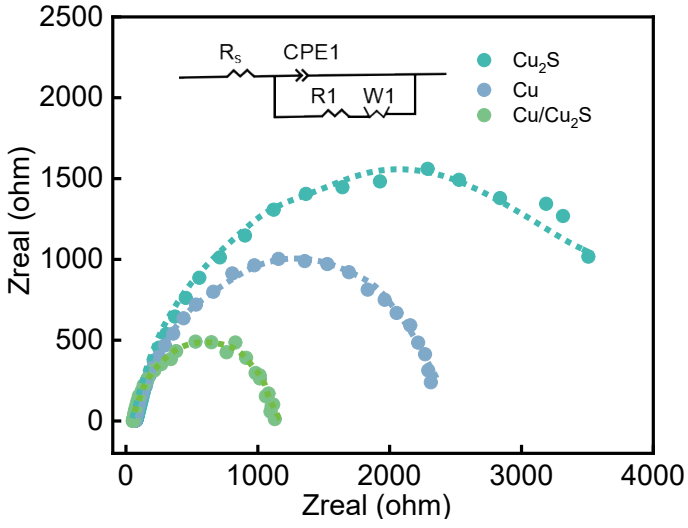

Figure S16 Electrochemical impedance spectroscopies of Cu-Cu_2S, Cu_2S and Cu.

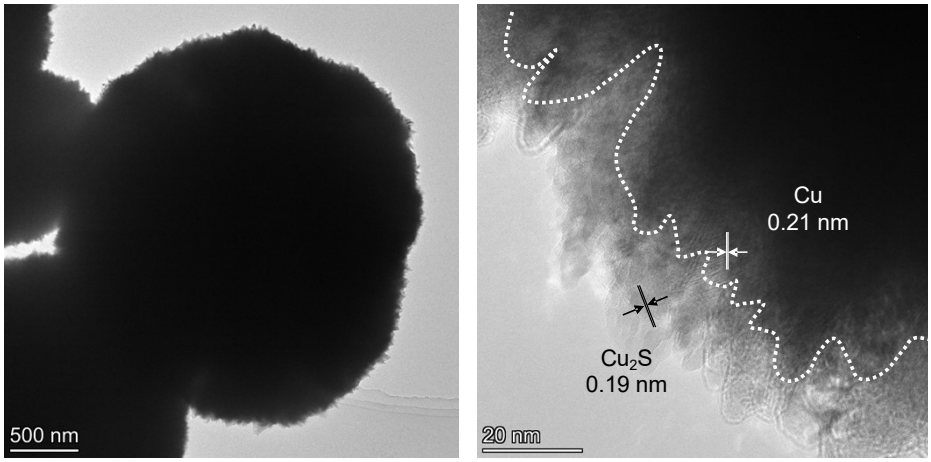

Figure S17 HR-TEM image of Cu-Cu_2S after stability test.

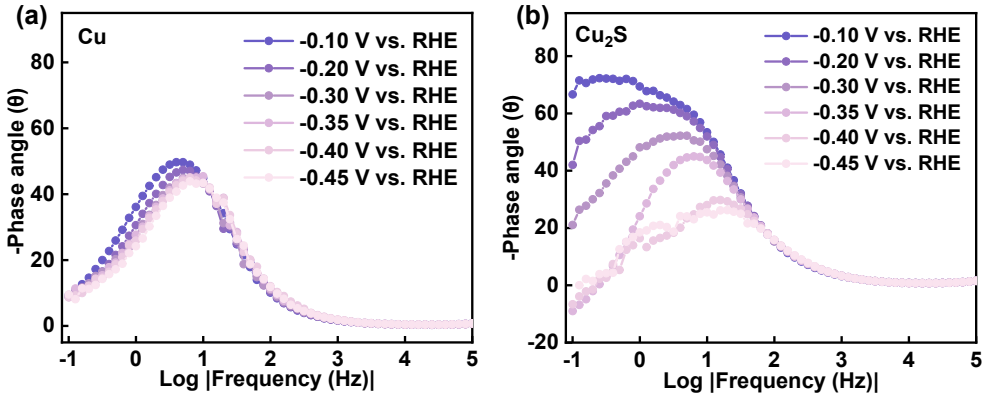

Figure S18 Electrochemical impedance spectroscopies of Cu (a) and Cu_2S (b) at different potentials.

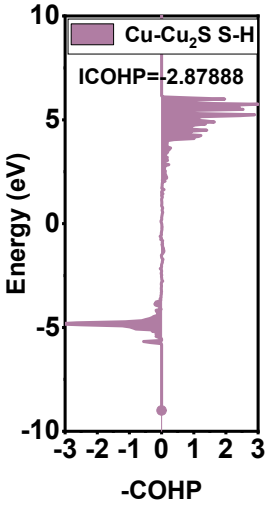

Figure S19 The Crystal Orbital Hamilton Population (COHP) of Cu-Cu_2S(S-H).

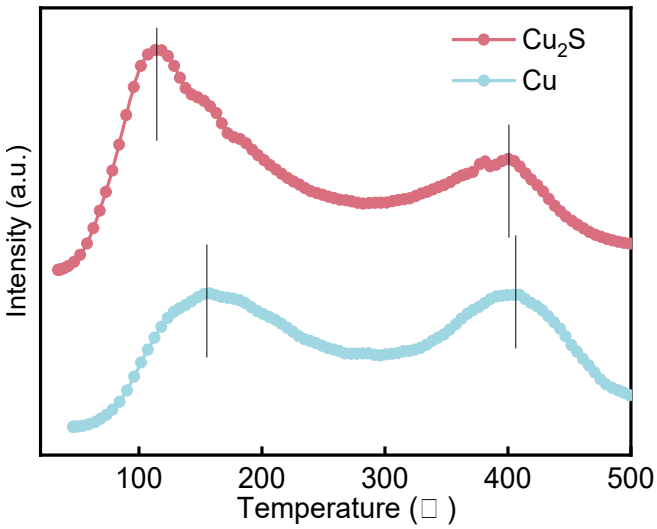

Figure S20 The CO_2-TPD curve of Cu and Cu_2S.

References

1. L. Pan, J. Wang, F. Lu, Q. Liu, Y. Gao, Y. Wang, J. Jiang, C. Sun, J. Wang and X. Wang, *Angewandte Chemie International Edition*, 2023, **62**, e202216835.
2. J. Geng, S. Ji, M. Jin, C. Zhang, M. Xu, G. Wang, C. Liang and H. Zhang, *Angewandte Chemie International Edition*, 2023, **62**, e202210958.
3. J. Liu, S. Zhang, Y. Jiang, W. Li, M. Jin, J. Ding, Y. Zhang, G. Wang and H. Zhang, *Chemical Communications*, 2024, **60**, 11592-11595.
4. H.-Q. Yin, Z.-S. Sun, Q.-P. Zhao, L.-L. Yang, T.-B. Lu and Z.-M. Zhang, *Journal of Energy Chemistry*, 2023, **84**, 385-393.
5. Y. Zhao, Y. Ding, W. Li, C. Liu, Y. Li, Z. Zhao, Y. Shan, F. Li, L. Sun and F. Li, *Nature Communications*, 2023, **14**, 4491.
6. M. Sun, G. Wu, J. Jiang, Y. Yang, A. Du, L. Dai, X. Mao and Q. Qin, *Angewandte Chemie International Edition*, 2023, **62**, e202301957.
7. M. Cong, Q. Liu, D. Wang, S. Hao, Z. Han, H. Xu, M. Guo, X. Ding and Y. Gao, *Applied Catalysis B: Environment and Energy*, 2024, **351**, 123941.
8. C. Lv, L. Zhong, H. Liu, Z. Fang, C. Yan, M. Chen, Y. Kong, C. Lee, D. Liu, S. Li, J. Liu, L. Song, G. Chen, Q. Yan and G. Yu, *Nature Sustainability*, 2021, **4**, 868-876.
9. S. Zhang, J. Geng, Z. Zhao, M. Jin, W. Li, Y. Ye, K. Li, G. Wang, Y. Zhang, H. Yin, H. Zhang and H. Zhao, *EES Catalysis*, 2023, **1**, 45-53.
10. C. Liu, H. Tong, P. Wang, R. Huang, P. Huang, G. Zhou and L. Liu, *Applied Catalysis B: Environmental*, 2023, **336**, 122917.
11. Y. Jeong, S. S. Naik, J. Theerthagiri, C. J. Moon, A. Min, M. L. Aruna Kumari and M. Y. Choi, *Chemical Engineering Journal*, 2023, **470**, 144034.